

SIMBIG: The First Cosmological Constraints from Non-Gaussian and Non-Linear Galaxy Clustering

CHANGHOON HAHN,^{1,*} PABLO LEMOS,^{2,3,4} LIAM PARKER,¹ BRUNO RÉGALDO-SAINTE-BLANCARD,⁴
MICHAEL EICKENBERG,⁴ SHIRLEY HO,⁵ JIAMIN HOU,^{6,7} ELENA MASSARA,^{8,9} CHIRAG MODI,^{4,5}
AZADEH MORADINEZHAD DIZGAH,¹⁰ AND DAVID SPERGEL^{5,1}

¹*Department of Astrophysical Sciences, Princeton University, Princeton NJ 08544, USA*

²*Department of Physics, Université de Montréal, Montréal, 1375 Avenue Thérèse-Lavoie-Roux, QC H2V 0B3, Canada*

³*Mila - Quebec Artificial Intelligence Institute, Montréal, 6666 Rue Saint-Urbain, QC H2S 3H1, Canada*

⁴*Center for Computational Mathematics, Flatiron Institute, 162 5th Avenue, New York, NY 10010, USA*

⁵*Center for Computational Astrophysics, Flatiron Institute, 162 5th Avenue, New York, NY 10010, USA*

⁶*Department of Astronomy, University of Florida, 211 Bryant Space Science Center, Gainesville, FL 32611, USA*

⁷*Max-Planck-Institut für Extraterrestrische Physik, Postfach 1312, Giessenbachstrasse 1, 85748 Garching bei München, Germany*

⁸*Waterloo Centre for Astrophysics, University of Waterloo, 200 University Ave W, Waterloo, ON N2L 3G1, Canada*

⁹*Department of Physics and Astronomy, University of Waterloo, 200 University Ave W, Waterloo, ON N2L 3G1, Canada*

¹⁰*Département de Physique Théorique, Université de Genève, 24 quai Ernest Ansermet, 1211 Genève 4, Switzerland*

ABSTRACT

The 3D distribution of galaxies encodes detailed cosmological information on the expansion and growth history of the Universe. We present the first cosmological constraints that exploit non-Gaussian cosmological information on non-linear scales from galaxy clustering, inaccessible with current standard analyses. We analyze a subset of the BOSS galaxy survey using SIMBIG, a new framework for cosmological inference that leverages high-fidelity simulations and deep generative models. We use two clustering statistics beyond the standard power spectrum: the bispectrum and a convolutional neural network based summary of the galaxy field. We infer constraints on Λ CDM parameters, Ω_b , h , n_s , Ω_m , and σ_8 , that are 1.6, 1.5, 1.7, 1.2, and $2.3\times$ tighter than power spectrum analyses. With this increased precision, we derive constraints on the Hubble constant, H_0 , and $S_8 = \sigma_8\sqrt{\Omega_m/0.3}$ that are competitive with other cosmological probes, even with a sample that only spans 10% of the full BOSS volume. Our H_0 constraints, imposing the Big Bang Nucleosynthesis prior on the baryon density, are consistent with the early time constraints from the cosmic microwave background (CMB). Meanwhile, our S_8 constraints are consistent with weak lensing experiments and similarly lie below CMB constraints. Lastly, we present forecasts to show that future work extending SIMBIG to upcoming spectroscopic galaxy surveys (DESI, PFS, *Euclid*) will produce leading H_0 and S_8 constraints that bridge the gap between early and late time measurements and shed light on current cosmic tensions.

Keywords: cosmological parameters from LSS — Machine learning — cosmological simulations — galaxy surveys

1. INTRODUCTION

The standard cosmological model (Λ CDM) has been remarkably successful at describing a wide range of cosmological observations, including the CMB (Page et al. 2003; Bennett et al. 2013; *Planck* Collab. et al. 2020a; Aiola et al. 2020; Dutcher et al. 2021), the large-scale structure (LSS; Bernardeau et al. 2002; Alam et al.

2017), distances to Type Ia supernovae (SN-Ia; Perlmutter et al. 1999; Riess et al. 1998; Scolnic et al. 2018; Brout et al. 2022), and the observed abundance of light elements (Schramm & Turner 1998; Steigman 2007; Iocco et al. 2009; Cyburt et al. 2016). Despite its success, Λ CDM has recently come under scrutiny from ‘cosmic tensions’, whose statistical significance has continued to persist with the latest observations (see Abdalla et al. 2022, for a review).

* changhoon.hahn@princeton.edu.com

The most statistically significant of the tensions is the ‘‘Hubble tension’’. It refers to the disagreement between the late-time measurements of the Hubble constant, H_0 , with early-time measurements inferred from CMB assuming Λ CDM (see [Freedman 2021](#); [Abdalla et al. 2022](#); [Kamionkowski & Riess 2022](#), for recent reviews). With the latest observations ([Riess et al. 2022](#); [Planck Collab. et al. 2020a](#)), the disagreement has a statistical significance of $>5\sigma$. Meanwhile, there is also an ‘‘ S_8 tension’’, which refers to the disagreement among measurements of the amplitude of the matter clustering, parameterized as $S_8 = \sigma_8 \sqrt{\Omega_m/0.3}$. Weak lensing analyses that probe LSS at $z \sim 0.5$ have systematically found S_8 values $\sim 2\sigma$ lower than expected from the best-fit CMB Λ CDM cosmology ([Troxel et al. 2018](#); [Asgari et al. 2021](#); [Amon et al. 2022](#); [Secco et al. 2022](#); [Dalal et al. 2023](#); [Sugiyama et al. 2023](#)). Their S_8 values are also lower than the recent constraints from CMB lensing, which probes LSS at higher redshifts, $z = 0.5 - 5$ ([Madhavacheril et al. 2023](#)). The H_0 and S_8 tension between late- and early-time constraints, have led a number of theoretical works to explore alternatives to Λ CDM (*e.g.* [Meerburg 2014](#); [Chudaykin et al. 2018](#); [Di Valentino et al. 2020](#); [Abellán et al. 2022](#); [Kamionkowski & Riess 2022](#)).

The 3D distribution of galaxies encodes cosmological information that addresses both tensions. We can compare the angular and physical scales of features in the galaxy distribution, *e.g.* Baryon Acoustic Oscillations (BAO; [Eisenstein et al. 1998](#); [Eisenstein et al. 2005](#); [Cole et al. 2005](#)), to compute physical distances and extract the Hubble constant (see [Ivanov & Philcox 2023](#), for a recent review). We can also measure the growth of structure from redshift-space distortions in the galaxy distribution to infer S_8 parameter. With these aims, spectroscopic galaxy surveys of the next decade, the Dark Energy Spectroscopic Instrument (DESI; [DESI Collaboration et al. 2016a,b](#); [Abareshi et al. 2022](#)), Subaru Prime Focus Spectrograph (PFS; [Takada et al. 2014](#); [Tamura et al. 2016](#)), the ESA *Euclid* satellite mission ([Laureijs et al. 2011](#)), and the Nancy Grace Roman Space Telescope (Roman; [Spergel et al. 2015](#); [Wang et al. 2022a](#)), will probe galaxies over unprecedented cosmic volumes. They will span >10 Gyrs of cosmic history, $0 < z \lesssim 3$, and precisely constrain H_0 and S_8 from the early- to late-times of the Universe.

To extract the cosmological information in galaxy distributions, current analyses primarily use the power spectrum, which captures all the information in a Gaus-

sian random field, as the summary statistic of galaxy clustering (*e.g.* [Alam et al. 2017](#); [Beutler et al. 2017](#); [Ivanov et al. 2020](#); [Chen et al. 2022](#); [Kobayashi et al. 2022](#)). Furthermore, they model the galaxy clustering using the perturbation theory (PT) of LSS and, as a result, are limited to large scales where deviations from linear theory are small ($k_{\max} \lesssim 0.2 h/\text{Mpc}$). However, recent studies have now established that there is additional cosmological information beyond these regimes. Analyses of the bispectrum, the first higher-order statistic, have shown that there is significant non-Gaussian information ([Gil-Marín et al. 2017](#); [Philcox & Ivanov 2022](#); [Ivanov et al. 2023](#)). Forecasts in [Hahn et al. \(2020\)](#) and [Hahn & Villaescusa-Navarro \(2021\)](#) have further shown that cosmological constraints improve by a factor of ~ 2 by analyzing the bispectrum down to non-linear scales ($k_{\max} = 0.5 h/\text{Mpc}$). Forecasts of other clustering statistics beyond the power spectrum find consistent improvements ([Massara et al. 2020, 2022](#); [Wang et al. 2022b](#); [Hou et al. 2022](#); [Eickenberg et al. 2022](#)).

Despite its promise, non-Gaussian cosmological information on non-linear scales cannot be robustly extracted using standard approaches. PT struggles to accurately model galaxy clustering beyond weakly non-linear scales. It also cannot model many of the newly proposed summary statistics (*e.g.* [Banerjee & Abel 2021](#); [Eickenberg et al. 2022](#); [Valogiannis & Dvorkin 2022](#); [Naidoo et al. 2022](#)). Observational systematics that significantly impact observed clustering are also a major challenge (*e.g.* [Ross et al. 2012, 2017](#)). Fiber collisions, for example, prevent galaxy surveys that use fiber-fed spectrographs (*e.g.* DESI, PFS) from successfully measuring redshifts of more than one galaxy within some angular scale. Even for the power spectrum, they cause significant bias on weakly non-linear scales, $k > 0.1 h/\text{Mpc}$ ([Guo et al. 2012](#)). While proposed corrections may be sufficient for the power spectrum ([Hahn et al. 2017](#); [Pinol et al. 2017](#); [Bianchi et al. 2018](#); [Smith et al. 2019](#)), no correction has yet been designed for statistics beyond the power spectrum.

With the SIMulation-Based Inference of Galaxies (SIMBIG), we go beyond the state-of-the-art galaxy clustering analyses. As we present in the first papers of the series ([Hahn et al. 2022](#) and [Hahn et al. 2023b¹](#)), SIMBIG is a forward modeling framework

¹ hereafter [H22a](#) and [H23](#)

that uses simulation-based inference² (SBI; see [Cranmer et al. 2020](#), for a review) with deep generative models from machine learning to perform highly efficient cosmological inference. SIMBIG leverages high-fidelity N -body simulations that accurately model non-linear galaxy clustering and includes observational effects. With this approach, [H22a](#) analyzed the power spectrum multipoles, $P_\ell(k)$, of galaxies³ in the Sloan Digital Sky Survey-III Baryon Oscillation Spectroscopic Survey (BOSS; [Eisenstein et al. 2011](#); [Dawson et al. 2013](#)) to demonstrate that we can robustly analyze the power spectrum down to non-linear scales. In this work, we go further and present the cosmological constraints that exploit *non-Gaussian* information and non-linear scales. We use two summary statistics of galaxy clustering beyond P_ℓ : the galaxy bispectrum and a field-level summary based on convolutional neural networks. We explore the cosmological implications of our constraints and address the H_0 and S_8 tensions.

We begin by briefly summarizing our methods in [Section 2](#). We present and discuss our cosmological results in [Section 3](#) and compare them to the literature. Lastly, we discuss future steps and prospects of extending SIMBIG to upcoming galaxy surveys in [Section 3.2](#).

2. METHODS

SIMBIG uses SBI to infer posteriors of Λ CDM cosmological parameters with only a forward model that can generate mock observations, *i.e.* the 3D galaxy spatial distribution. In this section, we briefly describe the forward model, the SBI methodology, the considered summaries of the galaxy distribution, and the validation of our analyses.

2.1. Forward Model

The SIMBIG forward model constructs simulated galaxy catalogs from QUIJOTE N -body simulations ([Villaescusa-Navarro et al. 2020](#)) run at different cosmologies in a Latin-hypercube configuration. Each simulation has a volume of $1 (h^{-1}\text{Gpc})^3$ and is constructed using 1024^3 cold dark matter particles initialized at $z = 127$ and gravitationally evolved until

² also known as “likelihood-free inference” (LFI) or “implicit likelihood inference” (ILI)

³ We used 109,636 galaxies in the Southern Galactic Cap (SGC) of the BOSS CMASS sample within $0.45 < z < 0.6$ and over $\sim 3,600 \text{ deg}^2$, which corresponds to roughly $\sim 10\%$ of the full BOSS volume.

$z = 0.5$. These high-resolution N -body simulations accurately model the clustering of matter down to non-linear scales beyond $k > 0.5 h/\text{Mpc}$. From the dark matter particles, halos are identified using the ROCKSTAR halo finder ([Behroozi et al. 2013](#)), which accurately determines the location of halos and resolve their substructure ([Knebe et al. 2011](#)). Afterwards, the halos are populated using the halo occupation distribution (HOD; *e.g.* [Berlind & Weinberg 2002](#)) framework, which provides a flexible statistical prescription for determining the number of galaxies as well as their positions and velocities within halos. SIMBIG uses a state-of-the-art 9-parameter HOD model that supplements the standard [Zheng et al. \(2007\)](#) model with assembly, concentration, and velocity biases for even more flexibility. From the HOD galaxy catalog, SIMBIG adds full BOSS survey realism by applying the survey geometry and observational systematics. The forward-modeled catalogs have the same redshift range and the angular footprint of our observed sample. In summary, the SIMBIG forward model aims to generate mock galaxy catalogs that are statistically indistinguishable from the observations. For further details, we refer readers to [H22a](#) and [H23](#).

2.2. Simulation-Based Inference

From the 20,000 forward-modeled galaxy catalogs, we use the SIMBIG SBI framework to infer posterior distributions of cosmological parameters, θ , for given a summary statistic, \mathbf{x} , of the observations: $p(\theta | \mathbf{x})$. The SBI in SIMBIG is based on neural density estimation (NDE) from deep generative models and uses “normalizing flow” ([Tabak & Vanden-Eijnden 2010](#); [Tabak & Turner 2013](#)). It enables cosmological inference with a limited number of simulated forward models so that we can extract cosmological information on small, non-linear, scales and using any statistic.

Among various normalizing flow architectures, SIMBIG uses Masked Autoregressive Flow (MAF; [Papamakarios et al. 2017](#)) and Neural Spline Flow (NSF; [Durkan et al. 2019](#)) models⁴. We train a flow that best approximates the posterior, $q_\phi(\theta | \mathbf{x}) \approx p(\theta | \mathbf{x})$, by minimizing the KL divergence between $p(\theta, \mathbf{x}) = p(\theta | \mathbf{x})p(\mathbf{x})$ and $q_\phi(\theta | \mathbf{x})p(\mathbf{x})$. In practice, we maximize the total log-likelihood $\sum_i \log q_\phi(\theta_i | \mathbf{x}_i)$ over the training set. We determine the training and architecture of

⁴ We use the normalizing flow implementation in `sbi` Python package ([Greenberg et al. 2019](#); [Tejero-Cantero et al. 2020](#)).

our flow through experimentation, tailored to each summary statistic.

The prior of our posterior estimate is set by the parameter distribution of our training set, which corresponds to a uniform prior over the cosmological parameters, $\{\Omega_m, \Omega_b, h, n_s, \sigma_8\}$, with ranges that extend well beyond the *Planck* posterior. For the HOD parameters, we use the conservative priors centered around previous HOD analyses of the BOSS CMASS sample.

2.3. Summary Statistics Beyond P_ℓ

We use two summary statistics of galaxy clustering beyond P_ℓ : the bispectrum (B_0) and a field-level summary using convolutional neural networks (CNNs). The bispectrum is the first higher-order statistic that measures the excess probability of finding galaxies in different triangle configurations over a random distribution. For a near-Gaussian galaxy distribution, the bispectrum extracts nearly all of its cosmological information (*e.g.* Fry 1994; Matarrese et al. 1997; Scoccimarro 2000). We also analyze the galaxy distribution at the field-level, using CNNs to perform massive data compression and extract maximally relevant features. By learning the relevant features, we aim to extract even more cosmological information than conventional summary statistics. We provide additional details on these summary statistics in Appendix A.1. We also refer readers to Hahn et al. (2023a) and Lemos et al. (2023) for further details.

2.4. Posterior Validation

For each summary statistic, we validate the trained q_ϕ in two steps. First, we perform a “NDE accuracy test” on a held-out subset of the training data, either using simulation-based calibration (Talts et al. 2020) or a “distance to random point” test (Lemos et al. 2023a). With this test, we check whether q_ϕ accurately estimates the posterior throughout the entire prior range of the cosmological parameters. Second, we assess the robustness of q_ϕ by applying it to the SIMBIG “mock challenge” simulations (H23). These simulations include three different sets of test simulations evaluated at some fiducial cosmology: 500 constructed using the same forward model as the training data, 500 constructed using a different halo finder and HOD model, and 1,000 constructed using a different N -body simulation and halo finder. We apply q_ϕ to the simulations and compare the resulting posteriors to their true parameter values. Since two of the test sets are constructed using different forward models than the training simulations, if the q_ϕ posteriors de-

rived from them are statistically consistent with the true values, we conclude that the q_ϕ is sufficiently robust.

3. RESULTS

We present the posteriors of the Λ CDM cosmological parameters for the B_0 (blue) and CNN (orange) SIMBIG analyses in Figure 1. In the right panels, we focus on the constraints on the growth of structure parameters: Ω_m and σ_8 . For comparison, we include the posteriors from the H22a SIMBIG (gray) and Ivanov et al. (2020) (black dashed) P_ℓ analyses. The Ivanov et al. (2020) constraints are inferred from roughly the same galaxy sample and is based on PT. In each of the contours, we mark the 68 and 95 percentiles of the posteriors. For all posteriors, we impose a Gaussian prior on $\omega_b = \Omega_b h^2 = 0.02268 \pm 0.00038$ from BBN studies (Aver et al. 2015; Cooke et al. 2018; Schöneberg et al. 2019), typically included in clustering analyses (*e.g.* Ivanov et al. 2020; Philcox & Ivanov 2022). We list the marginalized parameter constraints in Table 3.

Focusing first on $B_0(k_{123} < 0.5 h/\text{Mpc})$, we find that our Λ CDM constraints are significantly tighter yet consistent with P_ℓ constraints. Compared to the SIMBIG $P_\ell(k < 0.5 h/\text{Mpc})$ constraints, the SIMBIG B_0 constraints are 2.78, 3.17, 1.91, 1.77, and $1.53\times$ tighter for Ω_b , h , n_s , Ω_m , and σ_8 . Compare to the Ivanov et al. (2020) $P_\ell(k < 0.25 h/\text{Mpc})$ constraints, the B_0 constraints are 1.59, 1.51, 1.68, 1.17, and $2.04\times$ tighter for Ω_b , h , n_s , Ω_m , and σ_8 , respectively. The improvement on σ_8 is larger because Ivanov et al. (2020) does not include the non-linear scales ($0.25 < k < 0.5 h/\text{Mpc}$) included in the SIMBIG P_ℓ analyses.

Similarly, our constraints from the SIMBIG CNN analysis are significantly tighter yet consistent with the P_ℓ constraints. For Ω_b , h , n_s , Ω_m , and σ_8 , the CNN constraints are 2.51, 2.51, 1.46, 1.42, and $1.75\times$ tighter than the SIMBIG P_ℓ constraints. In comparison to the PT P_ℓ analysis, the Ω_b , h , n_s , and σ_8 constraints are 1.44, 1.20, 1.28, and $2.33\times$ tighter while the Ω_m constraint is slightly ($1.07\times$) broader.

Overall, the CNN and B_0 constraints are in excellent agreement. There is a slight offset in n_s ; however it is not statistically significant. The CNN constraints are slightly broader overall than B_0 except for σ_8 , even though the CNN aims to maximally extract the cosmological information in the galaxy field. This is in part due to the fact that, in practice, we limit the CNN’s

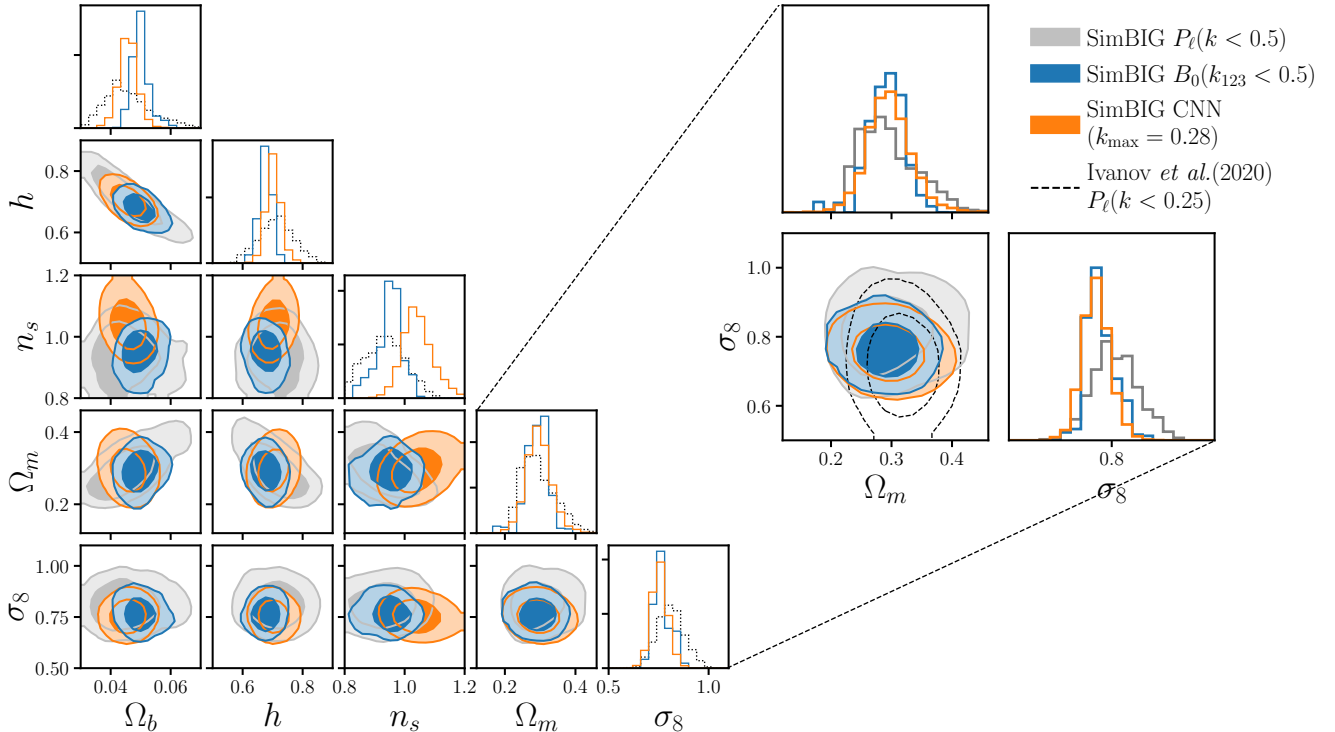


Figure 1. *Left:* Posteriors of cosmological parameters inferred from B_0 (blue) and CNN (orange) using SIMBIG. All posteriors include a ω_b prior from BBN studies. The contours mark the 68 and 95 percentiles. For comparison, we include the posterior from the SIMBIG P_ℓ analysis (gray). *Right:* We focus on the posteriors of Ω_m and σ_8 , the parameters that can be most significantly constrained by galaxy clustering. We include the posterior from the *Ivanov et al. (2020)* PT-based $P_\ell(k < 0.25 h/\text{Mpc})$ analysis for reference (black dashed). The SIMBIG B_0 and CNN constraints are significantly tighter yet consistent with P_ℓ constraints.

constraining power of the CNN to ensure robustness and generalizability (Appendix A.1).

Overall, the SIMBIG analyses beyond P_ℓ produce significantly tighter cosmological constraints than P_ℓ analyses. Taking the best constraints from the B_0 and CNN analyses, we improve Ω_b , h , n_s , Ω_m , and σ_8 by 1.59, 1.51, 1.68, 1.17, and 2.33 \times over the PT P_ℓ analysis. This firmly shows that there is substantial non-Gaussian cosmological information in galaxy clustering. Furthermore, our posteriors are in excellent agreement with previous galaxy clustering analyses that use an entirely different approach. This consistency serves as additional corroboration that SIMBIG provides a robust framework for analyzing clustering beyond P_ℓ .

3.1. Cosmic Tensions

Our tighter constraints on cosmological parameters enable us to also inform the S_8 and H_0 cosmic tensions. In Figure 2, we present the S_8 and H_0 posteriors from the SIMBIG B_0 (blue) and CNN (orange) analyses. For comparison, we also plot the posterior for the *Ivanov et al. (2020)* P_ℓ PT analysis (black dashed). We again include a ω_b prior from BBN studies. The S_8 and H_0

constraints from B_0 and CNN are consistent with each other (Table 3). Compared to *Ivanov et al. (2020)*, B_0 improves S_8 and H_0 constraints by 1.92 and 1.51 \times and the CNN improves the S_8 and H_0 by 1.83 and 1.20 \times .

Next, we compare our S_8 and H_0 posteriors to constraints in the literature from galaxy clustering and other cosmological probes (Figure 3). The constraints from the literature are selected from *Abdalla et al. (2022)*. In the left panel, we compare the SIMBIG S_8 constraints (black) to constraints from galaxy clustering (red), CMB (blue), weak lensing (purple), and multi-probe (brown) analyses. From galaxy clustering, we include the *Ivanov et al. (2020)* and *Kobayashi et al. (2022)* P_ℓ analyses of the CMASS-SGC sample. These analyses use nearly the same observational sample so their constraints are the most consistently comparable to the SIMBIG constraints⁵. We also include constraints from PT analyses of the full BOSS volume: *Philcox & Ivanov (2022)* and *Chen et al. (2022)*. *Philcox & Ivanov (2022)*

⁵ The galaxy sample in our SIMBIG analyses has a $\sim 30\%$ smaller footprint than the CMASS-SGC.

	Ω_m	σ_8	Ω_b	h	n_s	S_8	H_0
$P_\ell(k < 0.5)$	$0.287^{+0.059}_{-0.038}$	$0.808^{+0.068}_{-0.066}$	$0.044^{+0.009}_{-0.006}$	$0.713^{+0.056}_{-0.059}$	$0.935^{+0.070}_{-0.073}$	$0.797^{+0.107}_{-0.093}$	$71.255^{+5.615}_{-5.921}$
$B_0(k_{123} < 0.5)$	$0.297^{+0.020}_{-0.035}$	$0.763^{+0.054}_{-0.033}$	$0.050^{+0.003}_{-0.002}$	$0.676^{+0.018}_{-0.018}$	$0.952^{+0.035}_{-0.040}$	$0.757^{+0.048}_{-0.053}$	$67.556^{+1.801}_{-1.843}$
CNN	$0.295^{+0.036}_{-0.033}$	$0.753^{+0.040}_{-0.036}$	$0.046^{+0.003}_{-0.003}$	$0.702^{+0.024}_{-0.022}$	$1.039^{+0.053}_{-0.044}$	$0.746^{+0.055}_{-0.051}$	$70.199^{+2.387}_{-2.208}$

Table 1. Posteriors of Λ CDM cosmological parameters inferred from the power spectrum multipoles, the bispectrum monopole, and the CNN using SIMBIG. We present the median and 68 percentile uncertainties of the parameters. All posteriors include a ω_b prior from BBN.

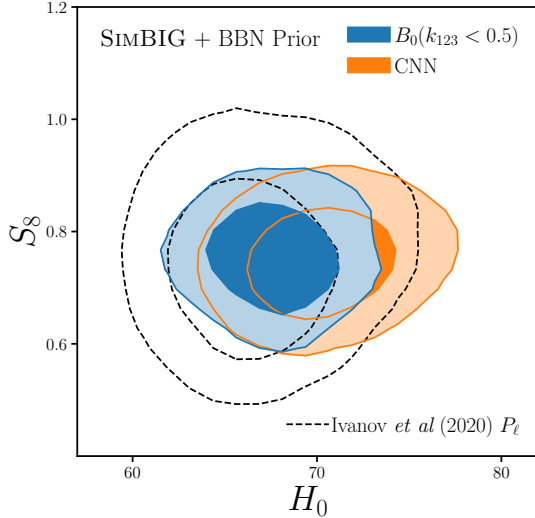


Figure 2. S_8 and H_0 posteriors for the SIMBIG B_0 (blue) and CNN (orange) analyses. We include the posterior from the Ivanov et al. (2020) P_ℓ analyses of CMASS-SGC for comparison (black dashed). All posteriors include a ω_b prior from BBN studies. With the B_0 and CNN, we infer consistent posteriors on S_8 and H_0 that are ~ 1.9 and $1.5\times$ tighter than the PT P_ℓ analyses. Our tighter constraints enable us to inform the S_8 and H_0 “tensions” found between cosmological probes in the early versus late Universe.

analyze both P_ℓ and B_0 and includes a BBN prior; Chen et al. (2022) analyze the pre- and post-reconstruction P_ℓ with fixed Ω_b and n_s . Despite only analyzing 10% of the total BOSS volume, our analyses produce S_8 constraints with comparable precision level to full volume analyses.

For CMB, we include constraints from: *Planck* TT,TE,EE+lowE with and without CMB lensing (*Planck* Collab. et al. 2020b); the Aiola et al. (2020) combined high- ℓ and low- ℓ measurements from the Atacama Cosmology Telescope (ACT) and the Wilkinson Microwave Anisotropy Probe (WMAP); and the ACT CMB lensing constraint combined with BAO (Madhavacheril et al. 2023). For weak lensing (WL), we include: the cosmic shear analysis of Kilo Degree Survey (KiDS; Asgari et al. 2021); the Asgari et al. (2020)

combined analysis of earlier KiDS data, VIKING data, and the Dark Energy Survey (DES) first year data; the DES analyses of the first (Troxel et al. 2018) and third year data (Amon et al. 2022; Secco et al. 2022); and the Hyper Suprime Cam (HSC) cosmic shear analysis (Dalal et al. 2023) and 3×2 pt analysis (Sugiyama et al. 2023) of the third year data. Lastly, we include multi-probe analyses that combine galaxy clustering and the cross-correlation with the *Planck* CMB lensing reconstruction (Krolewski et al. 2021; White et al. 2022).

Next, in the right panel of Figure 3, we compare the SIMBIG H_0 posteriors to constraints from a wide variety of cosmological probes: galaxy clustering (red), CMB (blue), SN-Ia (purple), and others (brown). From galaxy clustering, we include the Ivanov et al. (2020) CMASS-SGC analysis. Again, this is the analysis most consistent with our analyses. We also include the Philcox & Ivanov (2021), Chen et al. (2022), and Alam et al. (2017) analyses of the full BOSS volume. From CMB, we include constraints from WMAP (Hinshaw et al. 2013), *Planck* (*Planck* Collab. et al. 2020b), ACT (Aiola et al. 2020), and the South Pole Telescope (SPT; Dutcher et al. 2021). We also include H_0 constraints from distance ladder methods: SN-Ia calibrated using Cepheids from the SH0ES collaboration (Riess et al. 2022) and SN-Ia calibrated using the Tip of the Red Giant Branch (TRGB; Freedman 2021). Lastly, we include constraints from time-delay strong lensing (Denzel et al. 2021), the Tully-Fisher relation (Kourkchi et al. 2020), and gravitational wave standard sirens (Palmese et al. 2020).

The SIMBIG P_ℓ constraints are not precise enough to meaningfully inform the S_8 and H_0 tensions. However, the tighter constraints from the SIMBIG B_0 and CNN analyses provide interesting insights into the tension. For S_8 , the SIMBIG B_0 and CNN constraints are in good agreement with the weak lensing constraints and, thus, lower than the CMB constraints. Despite the differences, we emphasize that the SIMBIG constraints are statistically consistent with both CMB and weak lensing. For

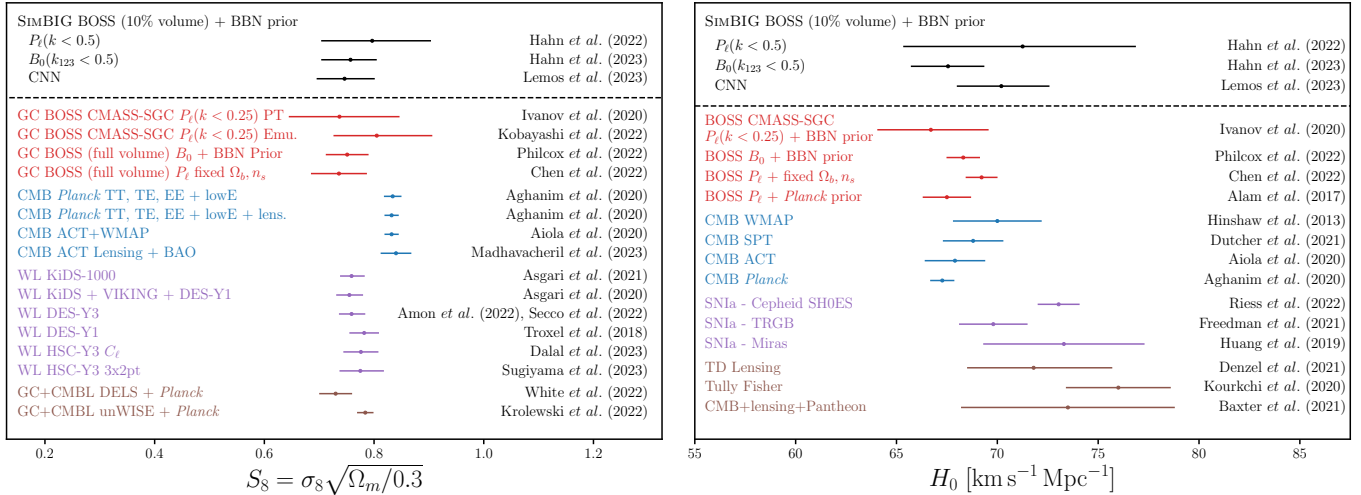


Figure 3. *Left:* Comparison of the SIMBIG S_8 constraints (black) to existing bounds in the literature. We include constraints from galaxy clustering (red), CMB (blue), weak lensing (purple), and multi-probe (brown) analyses. Despite only using 10% of the full BOSS volume, we derive S_8 constraints comparable to full BOSS P_ℓ analysis. Our S_8 constraints are in good agreement with weak lensing experiments and, thus, lie below the CMB constraints. *Right:* Comparison of the SIMBIG H_0 constraints (black) to the literature. We include constraints from galaxy clustering (red), CMB (blue), SN (purple), and other probes (brown). Our H_0 constraint from SIMBIG B_0 is in excellent agreement with *Planck*. We infer a higher H_0 with the CNN that is consistent with both *Planck* and SN-Ia constraints.

H_0 , the tighter constraints from SIMBIG B_0 and CNN are in good agreement with constraints from CMB and LSS. The B_0 constraint is in excellent agreement with *Planck* and, thus, is in tension with the SH0ES measurement. The CNN constraint is notably higher than the B_0 constraint and consequently reduces the tension with SH0ES. Nevertheless, it is statistically consistent with B_0 and *Planck*.

3.2. Future Steps and Upcoming Surveys

Despite only using 10% of the BOSS volume, we derive S_8 and H_0 constraints that are competitive with other cosmological probes and galaxy clustering analyses of the full BOSS volume. In short, our forward-modeling approach improves S_8 and H_0 constraints by ~ 2.0 and $1.5\times$ over the standard PT P_ℓ analysis. The improvement on S_8 is equivalent to applying the standard PT P_ℓ analysis to a galaxy sample *four times* the cosmic volume.

Yet, the improvement does not include *all* of the cosmological information that can be extracted using clustering statistics beyond P_ℓ . We require SIMBIG analyses to derive unbiased cosmological constraints for a suite of test simulations constructed with different forward models (Section 2.4). To meet this requirement for the CNN analysis, we use dropout, regularization, and SWA to reduce overfitting (Appendix A.1). These procedures

discard a substantial amount of cosmological information.

Solely for reference, in Figure 4 we present the Ω_m and σ_8 posterior for the CNN (red hatched) *if we relax our robustness requirement*. This is *not* a robust posterior; however, it illustrates that the CNN is capable of capturing significantly more cosmological information than the posteriors presented in this work. The non-robust CNN has $>2\times$ the precision of the robust CNN. In Figure 4, we also include posteriors derived from another summary statistic: the wavelet scattering transform (WST). The WST is set of descriptive statistics particularly suited for characterizing non-Gaussian fields. It is motivated by the structure of CNNs while being completely parameter-free. We exclude the WST analysis in our main comparison due to concerns about its robustness; however, the WST is capable of deriving constraints comparable to the B_0 analysis. For further details on the WST analysis, see Regalado-Saint Blancard et al. (2023).

The full constraining power of neither the CNN nor the WST can currently be robustly exploited. This is because these statistics identify cosmological imprints that are specific to our forward model. One way to robustly exploit these statistics is to use a more flexible and generalizable forward model that can describe the WST and CNN across the different test simulations. Alternatively,

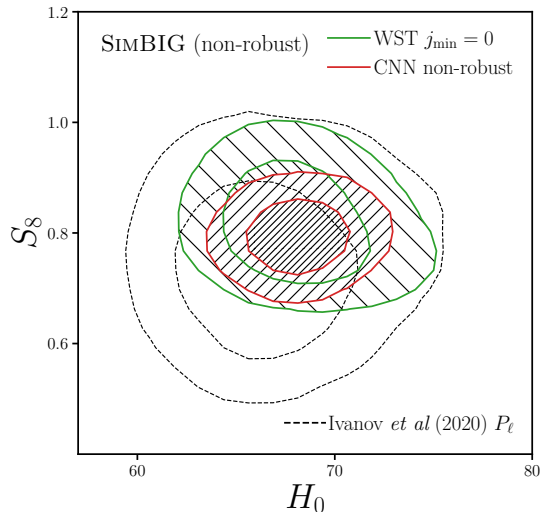


Figure 4. The H_0 and S_8 posterior for the CNN (red hatched) with *relaxed robustness requirements*. We also include the posterior from the SIMBIG WST analysis (green hatched). The posteriors are *not* robust; however, they illustrate the potential of the WST and CNN at capturing even more cosmological information than the posteriors presented above. The WST is capable of deriving constraints comparable to B_0 while the non-robust CNN can double the precision of the robust CNN constraints. In future work, we aim to extract some of this additional constraining power using SIMBIG with a more flexible and generalizable forward model and with summary statistics more robust to model misspecifications.

we can also construct clustering statistics more robust to model misspecification (*e.g.* Huang et al. 2023). Such an approach would learn the imprints of cosmological parameters while ignoring any model-specific features. In future work we will explore both approaches.

In future work, we will also extend SIMBIG to the next generation spectroscopic galaxy surveys. DESI will probe $14,000 \text{ deg}^2$ across $0 < z < 2.1$ with >40 million galaxies (Chaussidon et al. 2023; Hahn et al. 2022; Raichoor et al. 2023; Zhou et al. 2023). DESI has recently completed two out of its five years of observations. Meanwhile, the PFS Cosmology Survey will probe $1,200 \text{ deg}^2$ across $0.6 < z < 2.4$ with 4 million emission-line galaxies and is set to begin observations next year. Lastly, the *Euclid* spectroscopic survey (Euclid Collab. et al. 2022) will measure the redshift of about 30 million $H\alpha$ emitters across $15,000 \text{ deg}^2$ over $0.9 < z < 1.8$. It was recently launched in July 2023.

These surveys will probe enormous cosmic volumes in epochs without precise constraints on H_0 or S_8 from

other cosmological probes. We highlight this in Figure 5, where we present the forecasted 1σ precision levels of H_0 (top) and S_8 (bottom) constraints from applying SIMBIG to DESI, PFS, and *Euclid* (black). These forecasts are derived by scaling the SIMBIG constraints by $(V_{\text{survey}}/V_{\text{CMASS-SGC}})^{0.5}$. For H_0 , upcoming surveys will help bridge the gap between the late-time measurements from SN-Ia (SH0ES; red) and early-time measurements from the CMB (*Planck*; blue). H_0 constraints from other probes, *e.g.* time delay lensing, have significantly larger uncertainties and lie well outside the range of the figure. Similarly, for S_8 , DESI, PFS, and *Euclid* will bridge the gap between S_8 constraints from weak lensing surveys that probe low redshifts and from CMB lensing and CMB at high redshifts. The shaded regions represent the lensing efficiency kernel for weak lensing experiments ($0.1 < z < 0.7$; Amon et al. 2022) and the mass-map weights for CMB lensing ($0.5 < z < 5.0$; Madhavacheril et al. 2023).

SIMBIG can produce leading constraints on both S_8 and H_0 by more fully extracting the cosmological information of upcoming galaxy surveys. We note that the SIMBIG forecasts are conservative estimates that do not account for the fact that the DESI, PFS, and *Euclid* galaxy samples will have a higher number density than CMASS. Given their higher number density, we expect even larger gains from analyzing clustering beyond P_ℓ . With their precision levels and the extensive redshift range of DESI, PFS, and *Euclid*, future SIMBIG analyses will provide critical input into the cosmic tensions and potentially reveal new physics beyond the standard Λ CDM model.

4. SUMMARY

We present a comparison of SIMBIG cosmological constraints from analyzing galaxy clustering beyond the power spectrum: the bispectrum and a field-level summary statistic based on CNNs. SIMBIG provides a forward-modeling framework that uses simulation-based inference with normalizing flows to perform highly efficient cosmological inference using high-fidelity N -body simulations (H22a, H23). With SIMBIG, we extract non-Gaussian and non-linear cosmological information, currently inaccessible with standard PT analyses.

The SIMBIG B_0 and CNN analyses tightly constrain all Λ CDM parameters and, compared to a standard PT analysis of P_ℓ (Ivanov et al. 2020), improve Ω_b , h , n_s , Ω_m , and σ_8 constraints by 1.6, 1.5, 1.7, 1.2, and $2.3\times$. With these tighter constraints, the SIMBIG analyses can

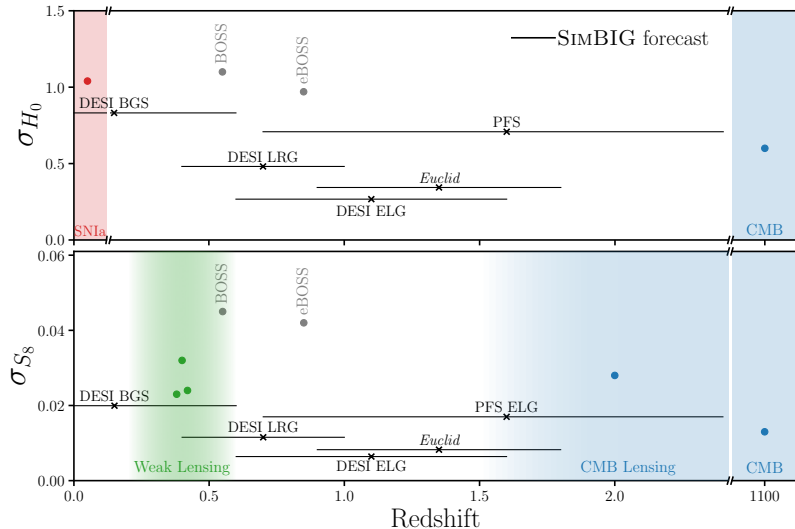


Figure 5. Expected 1σ precision level of H_0 (σ_{H_0} ; top) and S_8 (σ_{S_8} ; bottom) constraints from applying SIMBIG to upcoming galaxy surveys, DESI, PFS, *Euclid* (black). For DESI, we present SIMBIG forecasts for the different galaxy samples individually. The width of σ_{H_0} and σ_{S_8} marks the redshift range of each sample. We include constraints from SN-Ia (red), CMB and CMB lensing (blue), weak lensing (green), and previous BOSS/eBOSS P_ℓ analyses (gray), for comparison. Future SIMBIG analyses of DESI, PFS, and *Euclid* will have the precision and redshift range to provide key input into the H_0 and S_8 tensions and potentially reveal new physics beyond the standard Λ CDM model.

inform recent “tensions” between the early and late time measurements of S_8 and H_0 . Even with a subset set of the SDSS-III BOSS CMASS-SGC sample that corresponds to only $<10\%$ of the full volume, we derive S_8 constraints competitive with PT P_ℓ analyses of the full BOSS volume. Our S_8 constraint is statistically consistent with both CMB and weak lensing experiments. We also infer competitive H_0 constraints that are consistent with early universe constraints from CMB and other LSS analyses and in tension with late-time measurements.

In future work, we will focus on extending SIMBIG in two main avenues. First, we will increase the flexibility of our forward model in order to improve its robustness and generalizability. With a more robust forward model, we will use more constraining statistics that can improve cosmological constraints even further (Figure 4). We will also explore constructing new summary statistics that are simultaneously more sensitive to cosmological imprints and more robust to model misspecifications.

In addition, we will extend SIMBIG to upcoming spectroscopic galaxy surveys: DESI, PFS, and *Euclid*. These surveys will probe unprecedented volumes with >70 million galaxies. SIMBIG can produce leading constraints on both S_8 and H_0 across $0 < z < 2.4$ by more fully extracting the cosmological information from these

surveys (Figure 5). The SIMBIG analyses of these surveys will bridge the gap between the early- and late-time H_0 and S_8 constraints to provide key input into the tensions and potentially reveal deviations from the standard Λ CDM cosmology model.

ACKNOWLEDGEMENTS

It’s a pleasure to thank Peter Melchior, Uroš Seljak, Benjamin D. Wandelt, and the members of the Simons Collaboration on Learning the Universe⁶ for valuable discussions. We also thank Mikhail M. Ivanov and Yosuke Kobayashi for providing us with the posteriors used for comparison. This work was supported by the AI Accelerator program of the Schmidt Futures Foundation. JH has received funding from the European Union’s Horizon 2020 research and innovation program under the Marie Skłodowska-Curie grant agreement No 101025187. AMD acknowledges funding from Tomalla Foundation for Research in Gravity. The work reported on in this paper was substantially performed using the Princeton Research Computing resources at Princeton University, which is a consortium of groups led by the Princeton Institute for Computational Science and Engineering (PICSciE) and Office of Information Technology’s Research Computing.

APPENDIX

A. SUPPLEMENTARY INFORMATION

A.1. *Summary Statistics*

The bispectrum: $B(k_1, k_2, k_3)$, is the three-point correlation function in Fourier space and measures the excess probability of different triangle configurations (k_1, k_2, k_3) over a random distribution. In this work, we use the monopole of the bispectrum: $B_0(k_1, k_2, k_3)$. To measure B_0 , we use the redshift-space bispectrum estimator by [Scoccimarro \(2015\)](#). The estimator accounts for the survey geometry using a random catalog that has the same radial and angular selection functions as the observed catalog but with >4 million objects. For each galaxy, we include the [Feldman et al. \(1994\)](#) weights. For the observed galaxy sample, we also include angular systematic weights to account for stellar density and seeing conditions as well as redshift failure weights. We do not include weights for fiber collisions, since this effect is included in the SIMBIG forward model. We measure B_0 in triangle configurations defined by k_1, k_2, k_3 bins of width $\Delta k = 0.0105 h/\text{Mpc}$. In practice, we use the reduced bispectrum, $Q_0(k_1, k_2, k_3)$, which normalizes the bispectrum to reduce the dynamic range of B_0 . For $k_{\text{max}} = 0.5 h/\text{Mpc}$, Q_0 has 10,052 total triangle configurations.

CNN: Convolutional Neural Networks (CNNs) can be thought of as flexible, hierarchical, non-linear functions that can be optimized to extract relevant features from input images or, in this case, 3D galaxy fields. In this work, we use a 3D CNN to perform a step of massive data compression from the galaxy sample directly to the cosmological parameters. First, the galaxy distributions are meshed to $64 \times 64 \times 128$ voxels using cloud-in-cell mass assignment. The voxels have dimensions $\sim [11, 11, 11] h/\text{Mpc}$, which imposes a scale cut of $k < k_{\text{max}} = 0.28 h/\text{Mpc}$. We then train the CNN to accurately compress the galaxy field by minimizing the mean-squared-error between the network-predicted cosmological parameters and the true parameter values of SIMBIG training set using stochastic gradient descent (SGD). In addition, we also perform weight marginalization on the network using Stochastic Weight Averaging (SWA; [Maddox et al. 2019](#); [Wilson & Izmailov 2020](#)), to improve the generalizability of our CNN ([Lemos et al. 2023b](#)).

REFERENCES

- Abareshi, B., Aguilar, J., Ahlen, S., et al. 2022, Overview of the Instrumentation for the Dark Energy Spectroscopic Instrument, doi: [10.48550/arXiv.2205.10939](https://doi.org/10.48550/arXiv.2205.10939)
- Abdalla, E., Abellán, G. F., Aboubrahim, A., et al. 2022, Journal of High Energy Astrophysics, 34, 49, doi: [10.1016/j.jheap.2022.04.002](https://doi.org/10.1016/j.jheap.2022.04.002)
- Abellán, G. F., Murgia, R., Poulin, V., & Lavalley, J. 2022, PhRvD, 105, 063525, doi: [10.1103/PhysRevD.105.063525](https://doi.org/10.1103/PhysRevD.105.063525)
- Aiola, S., Calabrese, E., Maurin, L., et al. 2020, Journal of Cosmology and Astroparticle Physics, 2020, 047
- Aiola, S., Calabrese, E., Maurin, L., et al. 2020, JCAP, 2020, 047, doi: [10.1088/1475-7516/2020/12/047](https://doi.org/10.1088/1475-7516/2020/12/047)
- Alam, S., Ata, M., Bailey, S., et al. 2017, MNRAS, 470, 2617, doi: [10.1093/mnras/stx721](https://doi.org/10.1093/mnras/stx721)
- Amon, A., Gruen, D., Troxel, M. A., et al. 2022, PhRvD, 105, 023514, doi: [10.1103/PhysRevD.105.023514](https://doi.org/10.1103/PhysRevD.105.023514)
- Asgari, M., Tröster, T., Heymans, C., et al. 2020, A&A, 634, A127, doi: [10.1051/0004-6361/201936512](https://doi.org/10.1051/0004-6361/201936512)
- Asgari, M., Lin, C.-A., Joachimi, B., et al. 2021, A&A, 645, A104, doi: [10.1051/0004-6361/202039070](https://doi.org/10.1051/0004-6361/202039070)
- Aver, E., Olive, K. A., & Skillman, E. D. 2015, JCAP, 2015, 011, doi: [10.1088/1475-7516/2015/07/011](https://doi.org/10.1088/1475-7516/2015/07/011)
- Banerjee, A., & Abel, T. 2021, MNRAS, 500, 5479, doi: [10.1093/mnras/staa3604](https://doi.org/10.1093/mnras/staa3604)
- Behroozi, P. S., Wechsler, R. H., & Wu, H.-Y. 2013, The Astrophysical Journal, 762, 109, doi: [10.1088/0004-637X/762/2/109](https://doi.org/10.1088/0004-637X/762/2/109)
- Bennett, C. L., Larson, D., Weiland, J. L., et al. 2013, The Astrophysical Journal Supplement Series, 208, 20
- Berlind, A. A., & Weinberg, D. H. 2002, ApJ, 575, 587, doi: [10.1086/341469](https://doi.org/10.1086/341469)
- Bernardeau, F., Colombi, S., Gaztanaga, E., & Scoccimarro, R. 2002, Physics Reports, 367, 1, doi: [10.1016/S0370-1573\(02\)00135-7](https://doi.org/10.1016/S0370-1573(02)00135-7)
- Beutler, F., Seo, H.-J., Saito, S., et al. 2017, Monthly Notices of the Royal Astronomical Society, 466, 2242, doi: [10.1093/mnras/stw3298](https://doi.org/10.1093/mnras/stw3298)

⁶ <https://www.learning-the-universe.org/>

- Bianchi, D., Burden, A., Percival, W. J., et al. 2018, *Monthly Notices of the Royal Astronomical Society*, 481, 2338, doi: [10.1093/mnras/sty2377](https://doi.org/10.1093/mnras/sty2377)
- Brout, D., Scolnic, D., Popovic, B., et al. 2022, *ApJ*, 938, 110, doi: [10.3847/1538-4357/ac8e04](https://doi.org/10.3847/1538-4357/ac8e04)
- Chaussidon, E., Yèche, C., Palanque-Delabrouille, N., et al. 2023, *ApJ*, 944, 107, doi: [10.3847/1538-4357/acb3c2](https://doi.org/10.3847/1538-4357/acb3c2)
- Chen, S.-F., Vlah, Z., & White, M. 2022, *JCAP*, 2022, 008, doi: [10.1088/1475-7516/2022/02/008](https://doi.org/10.1088/1475-7516/2022/02/008)
- Chudaykin, A., Gorbunov, D., & Tkachev, I. 2018, *PhRvD*, 97, 083508, doi: [10.1103/PhysRevD.97.083508](https://doi.org/10.1103/PhysRevD.97.083508)
- Cole, S., Percival, W. J., Peacock, J. A., et al. 2005, *MNRAS*, 362, 505, doi: [10.1111/j.1365-2966.2005.09318.x](https://doi.org/10.1111/j.1365-2966.2005.09318.x)
- Cooke, R. J., Pettini, M., & Steidel, C. C. 2018, *ApJ*, 855, 102, doi: [10.3847/1538-4357/aaab53](https://doi.org/10.3847/1538-4357/aaab53)
- Cranmer, K., Brehmer, J., & Louppe, G. 2020, *Proceedings of the National Academy of Sciences*, 117, 30055, doi: [10.1073/pnas.1912789117](https://doi.org/10.1073/pnas.1912789117)
- Cyburt, R. H., Fields, B. D., Olive, K. A., & Yeh, T.-H. 2016, *Reviews of Modern Physics*, 88, 015004, doi: [10.1103/RevModPhys.88.015004](https://doi.org/10.1103/RevModPhys.88.015004)
- Dalal, R., Li, X., Nicola, A., et al. 2023, arXiv e-prints, arXiv:2304.00701, doi: [10.48550/arXiv.2304.00701](https://doi.org/10.48550/arXiv.2304.00701)
- Dawson, K. S., Schlegel, D. J., Ahn, C. P., et al. 2013, *The Astronomical Journal*, 145, 10, doi: [10.1088/0004-6256/145/1/10](https://doi.org/10.1088/0004-6256/145/1/10)
- Denzel, P., Coles, J. P., Saha, P., & Williams, L. L. R. 2021, *MNRAS*, 501, 784, doi: [10.1093/mnras/staa3603](https://doi.org/10.1093/mnras/staa3603)
- DESI Collaboration, Aghamousa, A., Aguilar, J., et al. 2016a, arXiv:1611.00036 [astro-ph]. <https://arxiv.org/abs/1611.00036>
- . 2016b, arXiv:1611.00037 [astro-ph]. <https://arxiv.org/abs/1611.00037>
- Di Valentino, E., Melchiorri, A., Mena, O., & Vagnozzi, S. 2020, *PhRvD*, 101, 063502, doi: [10.1103/PhysRevD.101.063502](https://doi.org/10.1103/PhysRevD.101.063502)
- Durkan, C., Bekasov, A., Murray, I., & Papamakarios, G. 2019, arXiv e-prints, arXiv:1906.04032, doi: [10.48550/arXiv.1906.04032](https://doi.org/10.48550/arXiv.1906.04032)
- Dutcher, D., Balkenhol, L., Ade, P., et al. 2021, *Physical Review D*, 104, 022003
- Dutcher, D., Balkenhol, L., Ade, P. A. R., et al. 2021, *PhRvD*, 104, 022003, doi: [10.1103/PhysRevD.104.022003](https://doi.org/10.1103/PhysRevD.104.022003)
- Eickenberg, M., Allys, E., Moradinezhad Dizgah, A., et al. 2022, *Wavelet Moments for Cosmological Parameter Estimation*
- Eisenstein, D. J., Hu, W., & Tegmark, M. 1998, *The Astrophysical Journal Letters*, 504, L57, doi: [10.1086/311582](https://doi.org/10.1086/311582)
- Eisenstein, D. J., Zehavi, I., Hogg, D. W., et al. 2005, *ApJ*, 633, 560, doi: [10.1086/466512](https://doi.org/10.1086/466512)
- Eisenstein, D. J., Weinberg, D. H., Agol, E., et al. 2011, *The Astronomical Journal*, 142, 72, doi: [10.1088/0004-6256/142/3/72](https://doi.org/10.1088/0004-6256/142/3/72)
- Euclid* Collab., Scaramella, R., Amiaux, J., et al. 2022, *A&A*, 662, A112, doi: [10.1051/0004-6361/202141938](https://doi.org/10.1051/0004-6361/202141938)
- Planck* Collab., Aghanim, N., Akrami, Y., et al. 2020a *Planck* Collab., Aghanim, N., Akrami, Y., et al. 2020b, *A&A*, 641, A6, doi: [10.1051/0004-6361/201833910](https://doi.org/10.1051/0004-6361/201833910)
- Feldman, H. A., Kaiser, N., & Peacock, J. A. 1994, *The Astrophysical Journal*, 426, 23, doi: [10.1086/174036](https://doi.org/10.1086/174036)
- Freedman, W. L. 2021, *ApJ*, 919, 16, doi: [10.3847/1538-4357/ac0e95](https://doi.org/10.3847/1538-4357/ac0e95)
- Fry, J. N. 1994, *PhRvL*, 73, 215, doi: [10.1103/PhysRevLett.73.215](https://doi.org/10.1103/PhysRevLett.73.215)
- Gil-Marín, H., Percival, W. J., Verde, L., et al. 2017, *Monthly Notices of the Royal Astronomical Society*, 465, 1757, doi: [10.1093/mnras/stw2679](https://doi.org/10.1093/mnras/stw2679)
- Greenberg, D. S., Nonnenmacher, M., & Macke, J. H. 2019, *Automatic Posterior Transformation for Likelihood-Free Inference*
- Guo, H., Zehavi, I., & Zheng, Z. 2012, *The Astrophysical Journal*, 756, 127, doi: [10.1088/0004-637X/756/2/127](https://doi.org/10.1088/0004-637X/756/2/127)
- Hahn, C., Eickenberg, M., Ho, S., & SIMBIG. 2023a Hahn, C., Scoccimarro, R., Blanton, M. R., Tinker, J. L., & Rodríguez-Torres, S. A. 2017, *Monthly Notices of the Royal Astronomical Society*, 467, 1940, doi: [10.1093/mnras/stx185](https://doi.org/10.1093/mnras/stx185)
- Hahn, C., & Villaescusa-Navarro, F. 2021, *Journal of Cosmology and Astroparticle Physics*, 2021, 029, doi: [10.1088/1475-7516/2021/04/029](https://doi.org/10.1088/1475-7516/2021/04/029)
- Hahn, C., Villaescusa-Navarro, F., Castorina, E., & Scoccimarro, R. 2020, *Journal of Cosmology and Astroparticle Physics*, 03, 040, doi: [10.1088/1475-7516/2020/03/040](https://doi.org/10.1088/1475-7516/2020/03/040)
- Hahn, C., Eickenberg, M., Ho, S., et al. 2022 Hahn, C., Wilson, M. J., Ruiz-Macias, O., et al. 2022, *DESI Bright Galaxy Survey: Final Target Selection, Design, and Validation*
- Hahn, C., Eickenberg, M., Ho, S., et al. 2023b, *JCAP*, 2023, 010, doi: [10.1088/1475-7516/2023/04/010](https://doi.org/10.1088/1475-7516/2023/04/010)
- Hinshaw, G., Larson, D., Komatsu, E., et al. 2013, *ApJS*, 208, 19, doi: [10.1088/0067-0049/208/2/19](https://doi.org/10.1088/0067-0049/208/2/19)
- Hou, J., Moradinezhad Dizgah, A., Hahn, C., & Massara, E. 2022, arXiv e-prints, arXiv:2210.12743. <https://arxiv.org/abs/2210.12743>
- Huang, D., Bharti, A., Souza, A., Acerbi, L., & Kaski, S. 2023, arXiv e-prints, arXiv:2305.15871, doi: [10.48550/arXiv.2305.15871](https://doi.org/10.48550/arXiv.2305.15871)

- Iocco, F., Mangano, G., Miele, G., Pisanti, O., & Serpico, P. D. 2009, *PhR*, 472, 1, doi: [10.1016/j.physrep.2009.02.002](https://doi.org/10.1016/j.physrep.2009.02.002)
- Ivanov, M. M., & Philcox, O. H. E. 2023, arXiv e-prints, arXiv:2305.07977, doi: [10.48550/arXiv.2305.07977](https://doi.org/10.48550/arXiv.2305.07977)
- Ivanov, M. M., Philcox, O. H. E., Cabass, G., et al. 2023, *PhRvD*, 107, 083515, doi: [10.1103/PhysRevD.107.083515](https://doi.org/10.1103/PhysRevD.107.083515)
- Ivanov, M. M., Simonović, M., & Zaldarriaga, M. 2020, *Journal of Cosmology and Astroparticle Physics*, 2020, 042, doi: [10.1088/1475-7516/2020/05/042](https://doi.org/10.1088/1475-7516/2020/05/042)
- Kamionkowski, M., & Riess, A. G. 2022, arXiv e-prints, arXiv:2211.04492, doi: [10.48550/arXiv.2211.04492](https://doi.org/10.48550/arXiv.2211.04492)
- Knebe, A., Knollmann, S. R., Muldrew, S. I., et al. 2011, *Monthly Notices of the Royal Astronomical Society*, 415, 2293, doi: [10.1111/j.1365-2966.2011.18858.x](https://doi.org/10.1111/j.1365-2966.2011.18858.x)
- Kobayashi, Y., Nishimichi, T., Takada, M., & Miyatake, H. 2022, *PhRvD*, 105, 083517, doi: [10.1103/PhysRevD.105.083517](https://doi.org/10.1103/PhysRevD.105.083517)
- Kourkchi, E., Tully, R. B., Anand, G. S., et al. 2020, *ApJ*, 896, 3, doi: [10.3847/1538-4357/ab901c](https://doi.org/10.3847/1538-4357/ab901c)
- Krolewski, A., Ferraro, S., & White, M. 2021, *JCAP*, 2021, 028, doi: [10.1088/1475-7516/2021/12/028](https://doi.org/10.1088/1475-7516/2021/12/028)
- Laureijs, R., Amiaux, J., Arduini, S., et al. 2011, arXiv e-prints, arXiv:1110.3193
- Lemos, P., Coogan, A., Hezaveh, Y., & Perreault-Levasseur, L. 2023a, arXiv preprint arXiv:2302.03026
- Lemos, P., Cranmer, M., Abidi, M., et al. 2023b, *Machine Learning: Science and Technology*, 4, 01LT01
- Lemos, P., Parker, L., & SIMBIG. 2023
- Maddox, W. J., Izmailov, P., Garipov, T., Vetrov, D. P., & Wilson, A. G. 2019, *Advances in neural information processing systems*, 32
- Madhavacheril, M. S., Qu, F. J., Sherwin, B. D., et al. 2023, arXiv e-prints, arXiv:2304.05203, <https://arxiv.org/abs/2304.05203>
- Massara, E., Villaescusa-Navarro, F., Ho, S., Dalal, N., & Spergel, D. N. 2020, arXiv:2001.11024 [astro-ph], <https://arxiv.org/abs/2001.11024>
- Massara, E., Villaescusa-Navarro, F., Hahn, C., et al. 2022, *Cosmological Information in the Marked Power Spectrum of the Galaxy Field*, doi: [10.48550/arXiv.2206.01709](https://doi.org/10.48550/arXiv.2206.01709)
- Matarrese, S., Verde, L., & Heavens, A. F. 1997, *MNRAS*, 290, 651, doi: [10.1093/mnras/290.4.651](https://doi.org/10.1093/mnras/290.4.651)
- Meerburg, P. D. 2014, *PhRvD*, 90, 063529, doi: [10.1103/PhysRevD.90.063529](https://doi.org/10.1103/PhysRevD.90.063529)
- Naidoo, K., Massara, E., & Lahav, O. 2022, *Monthly Notices of the Royal Astronomical Society*, doi: [10.1093/mnras/stac1138](https://doi.org/10.1093/mnras/stac1138)
- Page, L., Barnes, C., Hinshaw, G., et al. 2003, *The Astrophysical Journal Supplement Series*, 148, 39
- Palmese, A., deVicente, J., Pereira, M. E. S., et al. 2020, *ApJL*, 900, L33, doi: [10.3847/2041-8213/abaeff](https://doi.org/10.3847/2041-8213/abaeff)
- Papamakarios, G., Pavlakou, T., & Murray, I. 2017, arXiv e-prints, 1705, arXiv:1705.07057
- Perlmutter, S., Aldering, G., Goldhaber, G., et al. 1999, *The Astrophysical Journal*, 517, 565
- Philcox, O. H. E., & Ivanov, M. M. 2021, arXiv:2112.04515 [astro-ph, physics:hep-ex], <https://arxiv.org/abs/2112.04515>
- Philcox, O. H. E., & Ivanov, M. M. 2022, *PhRvD*, 105, 043517, doi: [10.1103/PhysRevD.105.043517](https://doi.org/10.1103/PhysRevD.105.043517)
- Pinol, L., Cahn, R. N., Hand, N., Seljak, U., & White, M. 2017, *Journal of Cosmology and Astroparticle Physics*, 2017, 008, doi: [10.1088/1475-7516/2017/04/008](https://doi.org/10.1088/1475-7516/2017/04/008)
- Raichoor, A., Moustakas, J., Newman, J. A., et al. 2023, *AJ*, 165, 126, doi: [10.3847/1538-3881/acb213](https://doi.org/10.3847/1538-3881/acb213)
- Regaldo-Saint Blancard, B., Eickenberg, M., & SIMBIG. 2023
- Riess, A. G., Filippenko, A. V., Challis, P., et al. 1998, *The astronomical journal*, 116, 1009
- Riess, A. G., Yuan, W., Macri, L. M., et al. 2022, *ApJL*, 934, L7, doi: [10.3847/2041-8213/ac5c5b](https://doi.org/10.3847/2041-8213/ac5c5b)
- Ross, A. J., Percival, W. J., Sánchez, A. G., et al. 2012, *Monthly Notices of the Royal Astronomical Society*, 424, 564, doi: [10.1111/j.1365-2966.2012.21235.x](https://doi.org/10.1111/j.1365-2966.2012.21235.x)
- Ross, A. J., Beutler, F., Chuang, C.-H., et al. 2017, *Monthly Notices of the Royal Astronomical Society*, 464, 1168, doi: [10.1093/mnras/stw2372](https://doi.org/10.1093/mnras/stw2372)
- Schöneberg, N., Lesgourgues, J., & Hooper, D. C. 2019, *JCAP*, 2019, 029, doi: [10.1088/1475-7516/2019/10/029](https://doi.org/10.1088/1475-7516/2019/10/029)
- Schramm, D. N., & Turner, M. S. 1998, *Reviews of Modern Physics*, 70, 303, doi: [10.1103/RevModPhys.70.303](https://doi.org/10.1103/RevModPhys.70.303)
- Scoccimarro, R. 2000, *ApJ*, 544, 597, doi: [10.1086/317248](https://doi.org/10.1086/317248)
- Scoccimarro, R. 2015, *Physical Review D*, 92, doi: [10.1103/PhysRevD.92.083532](https://doi.org/10.1103/PhysRevD.92.083532)
- Scolnic, D. M., Jones, D. O., Rest, A., et al. 2018, *ApJ*, 859, 101, doi: [10.3847/1538-4357/aab9bb](https://doi.org/10.3847/1538-4357/aab9bb)
- Secco, L. F., Samuroff, S., Krause, E., et al. 2022, *PhRvD*, 105, 023515, doi: [10.1103/PhysRevD.105.023515](https://doi.org/10.1103/PhysRevD.105.023515)
- Smith, A., He, J.-h., Cole, S., et al. 2019, *Monthly Notices of the Royal Astronomical Society*, doi: [10.1093/mnras/stz059](https://doi.org/10.1093/mnras/stz059)
- Spergel, D., Gehrels, N., Baltay, C., et al. 2015, *Wide-Field Infrared Survey Telescope-Astrophysics Focused Telescope Assets WFIRST-AFTA 2015 Report*
- Steigman, G. 2007, *Annual Review of Nuclear and Particle Science*, 57, 463, doi: [10.1146/annurev.nucl.56.080805.140437](https://doi.org/10.1146/annurev.nucl.56.080805.140437)

- Sugiyama, S., Miyatake, H., More, S., et al. 2023, arXiv e-prints, arXiv:2304.00705, doi: [10.48550/arXiv.2304.00705](https://doi.org/10.48550/arXiv.2304.00705)
- Tabak, E. G., & Turner, C. V. 2013, *Communications on Pure and Applied Mathematics*, 66, 145, doi: [10.1002/cpa.21423](https://doi.org/10.1002/cpa.21423)
- Tabak, E. G., & Vanden-Eijnden, E. 2010, *Communications in Mathematical Sciences*, 8, 217, doi: [10.4310/CMS.2010.v8.n1.a11](https://doi.org/10.4310/CMS.2010.v8.n1.a11)
- Takada, M., Ellis, R. S., Chiba, M., et al. 2014, *Publications of the Astronomical Society of Japan*, 66, R1, doi: [10.1093/pasj/pst019](https://doi.org/10.1093/pasj/pst019)
- Talts, S., Betancourt, M., Simpson, D., Vehtari, A., & Gelman, A. 2020, arXiv:1804.06788 [stat]. <https://arxiv.org/abs/1804.06788>
- Tamura, N., Takato, N., Shimono, A., et al. 2016, in *Ground-Based and Airborne Instrumentation for Astronomy VI*, Vol. 9908, eprint: arXiv:1608.01075, 99081M, doi: [10.1117/12.2232103](https://doi.org/10.1117/12.2232103)
- Tejero-Cantero, A., Boelts, J., Deistler, M., et al. 2020, *Journal of Open Source Software*, 5, 2505, doi: [10.21105/joss.02505](https://doi.org/10.21105/joss.02505)
- Troxel, M. A., MacCrann, N., Zuntz, J., et al. 2018, *PhRvD*, 98, 043528, doi: [10.1103/PhysRevD.98.043528](https://doi.org/10.1103/PhysRevD.98.043528)
- Valogiannis, G., & Dvorkin, C. 2022, *PhRvD*, 105, 103534, doi: [10.1103/PhysRevD.105.103534](https://doi.org/10.1103/PhysRevD.105.103534)
- Villaescusa-Navarro, F., Hahn, C., Massara, E., et al. 2020, *The Astrophysical Journal Supplement Series*, 250, 2, doi: [10.3847/1538-4365/ab9d82](https://doi.org/10.3847/1538-4365/ab9d82)
- Wang, Y., Zhai, Z., Alavi, A., et al. 2022a, *The Astrophysical Journal*, 928, 1, doi: [10.3847/1538-4357/ac4973](https://doi.org/10.3847/1538-4357/ac4973)
- Wang, Y., Zhao, G.-B., Koyama, K., et al. 2022b, *Extracting High-Order Cosmological Information in Galaxy Surveys with Power Spectra*, doi: [10.48550/arXiv.2202.05248](https://doi.org/10.48550/arXiv.2202.05248)
- White, M., Zhou, R., DeRose, J., et al. 2022, *JCAP*, 2022, 007, doi: [10.1088/1475-7516/2022/02/007](https://doi.org/10.1088/1475-7516/2022/02/007)
- Wilson, A. G., & Izmailov, P. 2020, *Advances in neural information processing systems*, 33, 4697
- Zheng, Z., Coil, A. L., & Zehavi, I. 2007, *The Astrophysical Journal*, 667, 760, doi: [10.1086/521074](https://doi.org/10.1086/521074)
- Zhou, R., Dey, B., Newman, J. A., et al. 2023, *AJ*, 165, 58, doi: [10.3847/1538-3881/aca5fb](https://doi.org/10.3847/1538-3881/aca5fb)